Evaluation of Physical and Durability Characteristics of New Headed Glass-Fiber-Reinforced-Polymer (GFRP) Bars for Concrete Structures

Brahim Benmokrane,[1] Hamdy M. Mohamed,[2] Allan Manalo,[3] and Patrice Cousin[4]

[1]**Corresponding author.** Professor of Civil Engineering and Tier-1 Canada Research Chair in Advanced Composite Materials for Civil Structures and NSERC Chair in FRP Reinforcement for Concrete Structures, Department of Civil Engineering, University of Sherbrooke, Quebec, Canada, J1K 2R1. Tel.: 1-819-821-7758.
Brahim.Benmokrane@usherbrooke.ca

[2]Postdoctoral Fellow, Department of Civil Engineering, University of Sherbrooke, Quebec, Canada
Hamdy.Mohamed@usherbrooke.ca

[3]Assistant Professor, Centre of Excellence in Engineered Fibre Composites, Faculty of Health, Engineering and Sciences, University of Southern Queensland, Toowoomba, Queensland 4350, Australia
Allan.Manalo@usq.edu.au

[4]Research Associate,
Department of Civil Engineering, University of Sherbrooke, Quebec, Canada
Patrice.Cousin@USherbrooke.ca

Abstract

This paper presents the results of a collaborative research project with Quebec's Ministry of Transportation and the Ontario's Ministry of Transportation, which aimed at characterizing a new type of headed glass-fiber-reinforced-polymer (GFRP) reinforcing bar and evaluating its suitability as internal reinforcement for concrete structures. To achieve these objectives, the project was implemented in three stages: (1) evaluation of the physical and mechanical properties; (2) determination of the pullout behavior in concrete; and (3) characterization of the long-term durability of the headed GFRP bars. A total of 57 specimens embedded in a 200 mm concrete cube were tested with the direct pullout test to investigate the effect of confinement, bar size, concrete compressive strength, and exposure conditions on the pullout behavior of the headed GFRP bars. Simultaneously, microstructural analyses and measurements of the physicochemical and mechanical properties were carried out on conditioned and unconditioned headed GFRP bars. The results show that the materials, geometry, and interface configuration of the head provided very good mechanical interlocking to the GFRP bars. Up to 63% and 53% of the guaranteed tensile strength of the straight GFRP bars were achieved for 15.9 mm and 19 mm diameter bars with headed ends, respectively. Scanning electron microscopy and differential scanning calorimetry showed no material changes in the head and bars after exposure to alkaline solution and freeze–thaw cycling. Exposure to the alkaline solution under sustained loading had the most detrimental effect, with the bar retaining 79.4% of its pullout strength. The results indicate that the tested headed GFRP bar has suitable mechanical and durability properties for use as reinforcement in concrete bridge components.

Keywords: Glass-fiber-reinforced polymer; headed bar; physical; mechanical; durability; freeze-thaw, alkaline environment, concrete, pullout strength.

INTRODUCTION

Fiber-reinforced-polymer (FRP) bars have been extensively used as internal reinforcement in different concrete structures as an alternative to steel reinforcement due to their noncorrosive nature. FRP materials in general offer many advantages over the conventional steel, including one-quarter to one-fifth the density of steel, neutrality to electrical and magnetic disturbances, and greater tensile strength. In the last decade, several field applications of FRP bars in marine structures, concrete bridge-deck slabs, bridge barriers, parking garages, and concrete pavement, as well as several experimental studies have supported the suitability of FRP rebars for structural use (Benmokrane et al. 2006; Manalo et al. 2014). Still, continuous research and development activities are being conducted around the world to comprehensively gain an understanding of the structural and mechanical behavior of FRP bars to ensure their wide acceptance in the construction industry (ACI 440.1R-15).

The bond characteristics of FRP bar is one of the most important parameters that control the design of FRP-reinforced concrete members. In structural concrete, the provisions for anchorage of reinforcement present detailing problems due to the required development lengths (Thompson et al. 2002). Accordingly, FRP bars are produced with different types of surface textures—such as sand coated, spiral wrapped, helical, ribbed, and indented—to promote bond and develop strength (Esfahani et al. 2013). Even if the bar's surface profile has been enhanced or a coating added, a long development length is needed in order to fully use the high tensile strength of FRP bars (Davalos et al. 2008). In some cases, bent FRP bars have been used to provide enough anchorage (CSA S6-2014, El-Salakawy et al., 2005). In such cases, however, the bent portion of the FRP bars have shown significantly lower tensile capacity than the straight portion because of the redirection and rearrangement of the fibers in the bend (Ahmed et al. 2010, Azimi et al. 2014). Moreover, bend dimensions may not fit within the dimensions of a member and may create congestion, making the element difficult

to construct. These issues have resulted in the development of FRP bars with a headed end to shorten the required development length and to develop the bar's high tensile capacity. Nevertheless, there is little guidance currently available for designing headed FRP bars.

While a significant amount of data is currently available on the durability and bond performance of FRP bars (ACI 440.1R-15), the durability of headed FRP bars, however, has yet to be investigated and understood. Davalos et al. (2008) indicated that bond durability plays a critical role in the long-term performance of concrete structures internally reinforced with FRP bars. Moreover, Bank et al. (1998) suggested that exposure to different environmental conditions affects the properties of the FRP bars as well as their bond strength with concrete. Clearly, the pullout strength of headed FRP bars exposed to different environmental conditions is important and should be determined for long-term performance assessment.

Recently, a research project was implemented by the University of Sherbrooke in collaboration with Quebec's Ministry of Transportation (MTQ) and Ontario's Ministry of Transportation (MTO) to assess the performance of a new type of headed glass-fiber-reinforced-polymer (GFRP) bar and to determine its suitability as internal reinforcement for concrete bridge elements and structures. As the head is made of thermoplastic matrix—a polymer that can be repeatedly softened by temperature increases and hardened by temperature decreases—a detailed investigation on the mechanical properties and durability of this material is warranted. CAN/CSA-S6 (2014) approved the use of thermoplastic materials as primary reinforcement in concrete only after they have proven durability and then were permitted for use as secondary reinforcement only if the matrix were susceptible to alkali degradation. Moreover, thermosetting polymers are preferred over thermoplastic polymers because of the lack of experience in the use of thermoplastics in civil structural applications. Thus, the project reported on herein was conducted in three stages to completely

characterize the physical, mechanical, and durability properties of the headed GFRP bars. In the first stage, the physical and chemical properties of the head and bar materials were determined. The pullout behavior of the headed GFRP bars in concrete was then investigated in the second stage to examine the effects of different parameters such as concrete confinement, concrete compressive strength, and bar diameter. In the third and final stage, the pullout strength and retention of headed GFRP bars when exposed to an alkaline solution, freeze–thaw cycles, and combined alkaline exposure and sustained loading was determined. Microstructural analyses and measurements of the physicochemical and mechanical properties were also carried out on conditioned and unconditioned headed GFRP bars. This paper presents the results of these studies. Understanding the behavior and performance of headed FRP bars is critical for their safe design and acceptance as reinforcement in concrete structures. This paper also provides the information needed to develop design guidelines and specifications for headed FRP bars.

THE HEADED GFRP BARS

The newly developed head is made of thermoplastic matrix reinforced with short glass fibers, while the GFRP bar is made of continuous E-glass fibers in a vinyl ester resin, as shown in Figure 1.a. This new product is manufactured by Pultrall (Thetford Mines, Quebec, Canada). The head has a special rib configuration to enhance the bond with concrete interface and was cast on the end of the GFRP bar at high temperature. The head is approximately 100 mm in length with a maximum outer diameter of 50 mm at the end, as shown in Figure 1.b. This wide wedge helps transfer a large portion of the load from the bar to the concrete and develop uniform stress along the head. Beyond this wedge, the head tapers in five steps to reach the outer diameter of the blank bar. This configuration is responsible for developing a stronger anchor system and avoiding splitting action near the head. This surface geometry was selected

after a number of trials and evaluations. Similarly, the bar ends were prepared with rounded grooves on the surface to increase mechanical interlock with the head, as shown in Figure 1.c.

Physical Characterizations

Two elements were considered in the physical characterization: sand-coated GFRP bars and molded thermoplastic heads (without the internal portion of the bar), as shown in Figure 2. Experimental tests as described in Table 1 were conducted on the GFRP bar samples and on the head samples to determine their physical properties. These properties are presented and discussed in the following subsections.

Material Composition

Pyrolysis testing was conducted to determine the material composition of the head anchor in accordance with ASTM D3171 (2011), *Procedure G*. The samples were weighed and heated to 550°C; the residual powder (filler) was then weighed. The pyrolysis test showed that the head is made of thermoplastic resin and very short glass fibers measuring a few hundred microns. It consists of 55% resin and 45% fibers by weight. According to the manufacturer, the resin is a polyphthalamide (PPA) with a melting point of around 300°C. Platt (2003) reported the typical mechanical properties of PPA.

The fibre content by weight of the sand coated GFRP bars is reported in Table 2 as provided by the manufacturer. The sand was excluded from the calculation of fibre content in the GFRP bars.

Water Absorption

The water uptake was determined according to ASTM D 570 (2010) for bars and heads. The measurement was conducted on bar samples containing sand. Since the sand particles may be removed during the immersion water, the specimens are dried and weighed after the test, if needed.

Three specimens from bars and heads were cut, dried, and weighed. They were then immersed in water at 50°C. The samples were removed from the water after 24 hours, surface dried, and weighed. Then, they were placed in water again until reaching full saturation, i.e. when the weight became constant. The samples were then dried at 100°C and weighed to determine the water content in weight percentage. The water-absorption rates of the head at 24 hours and at saturation was 0.48% and 1.11% by weight, respectively. These rates are slightly higher than that of the GFRP bar, which were measured at 0.11 and 0.44% by weight after 24 hours and at saturation, respectively. It should be noted that the specified limit of water absorption for FRP reinforcing bars in ACI 440.6M (2008) and CSA-S807 (2010) is 1% and 0.75% (high durability), respectively.

Coefficient of Thermal Expansion

The coefficients of transverse thermal expansion (CTE) at operating temperatures of the anchor head and sand-coated GFRP bar were measured with thermomechanical analysis (TMA) in accordance with ASTM E 831 (2012). The sand was excluded because the samples were taken from the core of the bar and the head. The values of CTE were 38×10^{-6}/°C for the anchor head and 22×10^{-6}/°C for the bar. The small difference in the coefficient of thermal expansion between the bar and anchor head will not induce any delamination problems.

Glass Transition Temperature

The glass transition temperature, T_g, was determined by differential scanning calorimetry (DSC) according to the ASTM E 1131-08 (2014) test method. Samples ranging from 30 to 40 mg were taken from the core of the GFRP bars and head. These samples were weighed and placed in an aluminum pan. The samples were then heated to 200°C in a nitrogen atmosphere at a heating rate of 20°C/min. The T_g obtained was 142°C and 116°C for the head and the GFRP bar, respectively. Both these T_g values are higher than the specified limit of 100°C in

CSA S807 (2010) and ACI 440.6M (2008). The head's measured T_g is also consistent with the reported T_g of 115 ^oC–130^oC for high-temperature molding PPA (ASTM D5336-15).

Optical Microscopy

An anchor head was cut longitudinally and each piece was observed under optical microscopy, revealing that the contact at the bar–head interface was very intact (Figure 2). The presence of grooves can also be distinguished in the figure; they were provided to increase the shear strength between the head and bar.

EXPERIMENTAL PROGRAM

An experimental investigation was carried out to evaluate the pullout behavior of the headed GFRP bars before and after exposure to different environmental conditions. The following sections provide a detailed description of the parameters considered in this study, types of conditioning, specimen preparation, and test setup, and instrumentation.

Parameters Considered

The test parameters considered in this study are concrete confinement, bar diameter, concrete compressive strength, and exposure conditions.

Confinement

The effect of concrete confinement on the pullout capacity of headed GFRP bars was evaluated on concrete blocks with and without transverse steel reinforcement. Ten concrete blocks without spiral reinforcement were prepared, as control specimens. On the other hand, mild-steel bars 3.2 mm in diameter were used as spiral reinforcement to confine the 50 concrete blocks where the headed bars were embedded.

Bar Diameter

Two different bar sizes were used: Nos. 5 and 6 GFRP bars (diameters of 15.9 mm and 19 mm, respectively). Table 2 gives the characteristic tensile strength and mechanical properties of these bars, as supplied by the manufacturer.

Concrete Compressive Strength

The concrete blocks were cast with normal-weight concrete with an average 28-day compressive strength of 35±0.8 and 47±0.5 MPa. Type 1 Portland cement was used for both concrete mixtures. These mixes were considered to investigate the effect of concrete compressive strength on the pullout capacity of the headed GFRP rebars.

Exposure Conditions

The headed GFRP bars were prepared and grouped according to the exposure conditions below.

Group A

Headed GFRP bars were cast without conditioning in concrete blocks to serve as control specimens. The effects of concrete confinement, concrete strength, and bar diameter on the pullout behavior of these headed GFRP bars were evaluated.

Group B

Three 15.9 mm diameter headed GFRP bars were directly immersed in alkaline solution (pH of 12.8) for 60 days at 60°C before casting in concrete blocks. The conditioning was conducted in accordance with ACI 440.3R-12 (2012), Test Method B.6, and CSA-S806-12 (2012), Annex O. During conditioning, the level of alkaline solution and pH level were checked periodically and new solution was added as necessary.

Group C

Three 15.9 mm diameter headed GFRP bars were subjected to 500 freeze–thaw cycles (-18°C and +4°C) according to ASTM C666/C666M−15, Procedure B (2015), in the MTQ laboratory. The specimens were sent to the University of Sherbrooke, cast in concrete blocks, then subjected to direct pullout loading.

Group D

Three 15.9 mm diameter headed GFRP bars were cast in concrete blocks and exposed to freeze–thaw cycles of +30°C and -30°C per day for 30 days. This exposure condition was requested by MTQ and MTO.

Group E

Three 15.9 mm diameter headed GFRP bars were cast in concrete blocks and then conditioned in alkaline solution (pH of 12.8) under sustained tensile loading at 60°C for 60 days. This conditioning is quite similar to ACI440.3R, Test Method B.6 (2012). In this method, moist concrete surrounds the headed GFRP bar. The concrete blocks were immersed in the alkaline solution in 300 × 300 × 300 mm PVC tanks. During the conditioning, the samples were set in a rigid-steel loading frame to induce a strain equal to 3000 microstrains (CSA-S806-12, 2012). The test frames were designed so as not to induce torsional stress in the samples. The imposed strain was controlled by glued stoppers and was checked daily. Similarly, the temperature was monitored during the 120 days of conditioning. Figure 3 shows the test setup and schematic diagram of the headed GFRP bars conditioned in the alkaline solution under sustained loading.

Specimens Details

A total of 57 headed GFRP bars were prepared and tested to evaluate the effects of the different parameters considered in this study. Table 3 provides details of the specimens. The different specimens were designated according to conditioning type, bar number, concrete compressive strength, the presence (S) or absence (N) of confinement, and the specimen's number in the group. For example, specimen A-5-35-S-1 was the first specimen in the unconditioned headed GFRP bar group embedded in a concrete block with a compressive strength of 35MPa and spiral reinforcement.

Casting of Concrete Blocks

The headed FRP bars were centered and adjusted vertically in a wooden form measuring 200 × 200 × 200 mm. The load was intended to be resisted only by the head, so debonding tubes were attached to the headed GFRP bars starting from the end of the head up to 200 mm along the bar. For the confined specimens, the spiral reinforcement was inserted in the form at a pitch of 25 mm along the block's depth.

The concrete was placed in three layers of approximately equal thickness, and each layer was compacted 25 times with a 16 mm diameter tamping rod. After molding, the specimens were cured for 24 h by covering them with a plastic sheet to prevent moisture loss. The molds were then removed, and the specimens in groups A, B, and C were stored for 27 days in a moist room. During this period, water was sprayed daily to maintain moisture on the surfaces at all times. On the other hand, the specimens in groups D and E were subjected to the specified type of conditioning after mold removal. At least six 150 × 300 mm cylinders were also prepared for each concrete batch and cured under the same conditions as the control specimens. The concrete compressive strengths of these cylinders were determined at 28 days.

Test Setup and Instrumentation

Before testing, the free end of the GFRP bar was anchored in steel tubes filled with Bristar 10 cement as an adhesive. The concrete block was also attached with a closed steel-plate frame to confine and delay the splitting of the concrete. The specimens were then tested on a 1000 kN capacity BALDWIN machine (as shown in Fig. 4) under direct pullout testing according to the procedures in ACI 440.3R (2012). The loading rate was 2.0 kN/s and applied by manually controlling the hydraulic pump. The load was increased until the headed GFRP bar or concrete block failed. The load was measured with the machine's electronic load cell, which was connected to a data-acquisition system. After the testing, the concrete blocks that were not broken were carefully cut into halves to observe the anchor head's condition.

TEST RESULTS AND OBSERVATIONS

Mode of Failure

ACI 440.1R (2015) and Benmokrane et al. (2002) mentioned that pullout and splitting are the two dominant failure modes expected with GFRP rebars in concrete. Whether one or the other occurs depends on the confinement around the bars, concrete cover and strength, and bar embedment length (Harajli and Abouniaj 2010). In our study, four different types of failure were observed for the tested headed GFRP bars embedded in concrete: concrete breakout (CB); concrete splitting followed by head breakout and bar pullout (CSH); bar slippage from the head (BSH); and bar slippage due to shear failure of the grooves (BSG). All these modes of failure were explosive and combined with a sudden drop in the pullout capacity. The following presents a brief description of the different modes of failure observed:

(1) Concrete blowout (CB)

This type of failure is characterized by the breaking of the concrete block in three or more pieces, while the headed GFRP bar remains intact or with minimal damage near the end of the head (Figure 5a). When the head bears against the surrounding concrete during testing, the concrete tends to slide up along the head surface, causing blowing out of the side cover of the concrete block. In this case, the splitting resistance of the concrete blocks governs the level of pullout capacity of the headed GFRP bars. This mode of failure occurred exclusively with the headed GFRP bars embedded in a concrete block without spiral reinforcement.

(2) Concrete splitting followed by head breakout and then bar slippage (CSH)

This type of failure occurred when the friction between the head and the bar and between the head and the concrete prevented the headed GFRP bar from pulling out of the concrete block. The forward movement of the headed GFRP bars, however, caused splitting cracks to propagate from the head to the concrete surface. Typically, face and side splitting was observed on the concrete blocks. The confining stress provided by the spiral reinforcement

prevented the concrete from breaking out. At high load, the head's material strength was exceeded, causing it to break. This was followed by bar slippage as the bar lost some interlocking capacity at the surfaces between the bar and the head (Figure 5b). CSH occurred mainly for the unconditioned headed GFRP bars that were cast in concrete blocks with spiral steel reinforcement.

(3) Bar slippage from the head, BSH

The headed GFRP bars conditioned under exposures B, C and D as well as some of the unconditioned specimens failed by bar slippage from the head (BSH) without any splitting or cracking in the concrete block. In this type of failure, the head remained completely intact in the concrete block, although the GFRP bar had been pulled out. The grooves on the bar surface are clearly visible in Figure 5c, but the grooves on the head have suffered some damage, indicating that the bar slippage occurred because the longitudinal bond stress exceeded the shear strength between the GFRP bars and head. In other words, the failure due to the bar slippage from the head (BSH) occurred due to groove failure in the head, while the grooves on the bar surface remained mostly intact, as shown in Figure 5c.

(4) Bar slippage due to shear failure of the grooves (BSG)

Bar slippage as a result of the shear failure of the grooves was observed for the headed GFRP bars that were conditioned in alkaline solution (pH of 12.5) at 60°C under sustained tensile loading for 60 days (Group E). As can be clearly seen in Figure 5d, in this type of failure, the grooves on the bar surface inserted into the head were worn completely smooth. Clearly, the shear strength between the concrete and head wedges had to exceed the strength of the bar–head interface for this type of failure to occur. The bar slippage in both BSH and BSG indicates that the degradation of the bond (if any) between the concrete and head resulting from degradation of the concrete and bar properties did not affect the measured pullout strength, as the failure occurred solely at the bar and head interface.

Pullout-Load Capacity

Table 3 also gives the experimental results for the pullout capacity of the unconditioned and conditioned headed GFRP bars. Failure was defined as the point of maximum pullout load. The corresponding average tensile stress developed by the GFRP bar was also calculated by dividing the failure load to the nominal cross-sectional area of the bar. These tables also provide the percentage of the maximum nominal stress to that of the guaranteed tensile strength as well as the typical type of failure observed for each test. The experimental results also evidence a slightly higher failure load for samples failing from BSH rather than CSH. This observation further confirms the good bond between the head and bars. Due to concrete splitting from CSH, the load to pull the headed bars out of the concrete block becomes lower than from BSH as the confinement provided by concrete was lower.

ANALYSIS AND DISCUSSION

This section presents the analysis and discussion of the effects of the various parameters investigated on the pullout behavior of the headed GFRP bars. The pullout behavior and retention after exposure to different environmental conditions are also presented.

Effect of Steel Spiral

Cosenza et al. (1997) indicated that bond strength was highly dependent on concrete confinement. Harajli and Abouniaj (2010) further suggested that adding confinement reinforcement such as transverse steel would result in a sizable increase in the bond strength of GFRP bars. A similar trend was observed herein. The average pullout load for the headed GFRP bars embedded in concrete blocks without steel spirals was 122.7 kN and 149.5 kN for the 15.9 and 19 mm diameter bars, respectively. In the case of the spirally reinforced concrete blocks, the levels of pullout load were 139.8 kN and 171.7 kN, respectively, representing a 13% to 15% increase.

343 Incorporating spiral reinforcement had an obviously positive effect on failure behavior.
344 The concrete blocks without steel spirals failed by concrete blowout. Clearly, the concrete
345 blocks used had inadequate confining action to minimize the risk of breaking the concrete due
346 to the very high force needed to pull the headed GFRP bar out of the concrete block. As a
347 result, the headed GFRP bar was not able to achieve its maximum pullout capacity. In
348 comparison, providing spiral reinforcement improved the pullout capacity by restraining the
349 concrete block breakout and by confining the concrete underneath the head, thereby
350 improving the bearing capacity. The headed GFRP bars embedded in concrete failed
351 primarily as the result of the splitting of the concrete blocks, followed by head breakage;
352 some specimens failed due to bar slippage.

353 **Effect of Bar Diameter**

354 The effect of bar diameter was evaluated by comparing the average tensile stress developed
355 by the GFRP bars. The tensile stress measured in the 15.9 mm diameter headed GFRP bars in
356 35 MPa concrete was 699.5 MPa (139.8 kN), compared to 602.6 MPa (171.7 kN) for the
357 19 mm diameter bars. On the other hand, the tensile-stress measurements for the 15.9 mm and
358 19 mm diameter headed GFRP bars in 47 MPa concrete were 750.0 MPa (148.5 kN) and
359 626.9 MPa (178.6 kN), respectively. This represents decreases of 14% and 16% in the
360 developed level of stress or pullout resistance as the bar diameter increased. Benmokrane et
361 al. (1996) indicated that the average bond stress in FRP bars decreased as bar diameter
362 increased. The same conclusion was arrived at with ribbed GFRP bars with headed ends
363 (Islam et al. 2015). While our study revealed a similar trend, the reduced pullout capacity
364 cannot be directly correlated to the difference in bar diameter, as only the head was embedded
365 in the concrete block.

366 The pullout capacity of the headed GFRP bars relies to a great extent on the head bearing
367 against the concrete with some contribution from the shear resistance of the concrete along

368 the wedge surface. As the head geometry was the same for both the 15.9 mm and 19 mm
369 diameter bars, the shear friction along the wedge surface can be considered to be equal. On
370 the other hand, the head's projected bearing area on the concrete was different. Obviously, a
371 bigger diameter bar will result in a smaller bearing area than with a smaller diameter bar, as
372 the larger area is deducted from the head's total projected area. Thus, it can be concluded that
373 the lower pullout capacity of the 19 mm diameter headed GFRP bar compared to that of the
374 15.9 mm one is due to the lower net bearing area of the head. Ozbolt et al. (2007) made
375 similar observations, indicating that higher resistance can be obtained for anchor bolts with
376 higher bearing areas.

377 All the specimens in this study—that is, for both bar diameters and concrete compressive
378 strengths (35MPa and 47 MPa)—failed due to the concrete splitting, followed by head
379 breakout and bar slippage. This shows that the head size considered is sufficient to ensure
380 adequate bond between the concrete and head and to develop high tensile stress in the GFRP
381 bars.

382 **Effect of Concrete Strength**

383 The average pullout capacities of the 15.9 mm diameter headed GFRP bars embedded in 35
384 and 47 MPa concrete with spiral reinforcement were 138.5 kN and 148.5 kN, respectively.
385 The corresponding values for the 19 mm diameter headed bars were 171.7 and 178.6 kN.
386 These test results indicate that the pullout strength of the headed GFRP bars in the concrete
387 with 35 MPa compressive strength were 4% to 6% lower than those embedded in the 47 MPa
388 concrete. This insignificant difference in measured pullout capacities between the two
389 compressive strengths agrees with the findings of Tighiouart et al. (1998). These authors
390 concluded that the strength of the bond between GFRP bars and concrete did not increase
391 with increased concrete compressive strength. Okelo and Yuan (2005) also suggested that the
392 average bond strength could be assumed to be proportional to the square root of the

compressive strength of concrete. Based on this relation, the difference between 47 MPa and 36 MPa is only 14%. Accordingly, the almost similar pullout capacities measured could be because the two compressive strengths were too close in value for the anticipated increase to become evident. Moreover, the pullout capacity of the headed GFRP bars was governed by the concrete blocks resisting splitting; therefore, the concrete's tensile strength (not the compressive strength)—which was roughly 10% of the compressive strength—was the governing factor.

The nearly identical pullout loads for the two concrete compressive strengths can be correlated to the observed failure mechanism. When the concrete blocks were confined by the steel spiral, GFRP bar final failure was governed by head breakout, followed by bar slippage.

Effect of Exposure to an Alkaline Environment

The average pullout load measured for the headed GFRP bars exposed to the alkaline environment was 129.1 kN. This is almost 7% lower than that of the unconditioned specimens. The lower pullout strength recorded with this exposure condition could be due to absorbed moisture at the bar–head interface, which would weaken shear strength. This is supported by the observed failure behavior, wherein all the specimens exposed to the alkaline environment failed by bar slippage with the grooves still intact. Moreover, the lower pullout capacity for the headed GFRP bars is very minimal because the traditional environmental aging performed through immersion in a simulated concrete pore solution is much harsher than an actual concrete environment. The specimens evidenced strength retention of more than 93% after exposure to the alkaline solution for 60 days at 60^{o}C. This result is very promising as Al-Dulaijian et al. (2001) found that an alkaline environment at high temperature is a condition that could adversely affect the bond strength between GFRP bars and concrete. The 7% lower pullout capacity of the headed GFRP bars when exposed to the alkaline solution is significantly lower than the 20% loss in bond strength observed by

Davalos et al (2008), in whose study the GFRP bars were embedded in concrete in water at room temperature and 60^{o}C.

Effect of Exposure to Freeze–Thaw Cycles at -18 ^{o}C to 4^{o}C

The headed GFRP bars exposed to 500 freeze–thaw cycles at -18^{o}C to +4^{o}C failed at an average pullout load of 132.9 kN, representing nearly 96% retention of the pullout capacity of the unconditioned specimens. The small reduction in the pullout strength due to rapid freezing in air and thawing in water supports the findings by several researchers that this exposure condition has no significant effect on bond strength. Mashima and Iwamoto (1993) observed no change in the strength of the bond between GFRP bars and concrete even after a high number of freeze–thaw cycles. Homman and Sheikh (2000) found that freeze–thaw cycles without the presence of moisture do not significantly affect the mechanical properties of FRP rods. Micelli and Nanni (2004) did not observe any significant damage or decrease in the mechanical properties of GFRP bars after 200 freeze–thaw cycles (-18 to 4^{o}C). Alves et al. (2011) reported similar findings when they investigated the bond strength of GFRP bars in concrete subjected to 250 freeze–thaw cycles (-25^{o}C to 15^{o}C). In fact, these authors concluded that the freeze–thaw cycles could increase the strength of the bond between GFRP bars and concrete because the bar cross-sectional area could be greater due to absorbed moisture and thereby enhance frictional resistance. The almost 4% lower pullout strength, however, could be due to head and bar expansion and contraction caused by temperature cycling, which could affect the shear strength at the interface.

Effect of Exposure to Freeze – Thaw Cycles at -30^{o}C to 30^{o}C

The headed GFRP bars exposed to freeze–thaw cycles at -30 to +30^{o}C sustained a maximum load of 123.1 kN before failure. This represents an 88.9% retention of the pullout strength of the control specimens. The 11% lower pullout capacity of the headed GFRP bars exposed to freeze–thaw cycles at +30^{o}C to -30^{o}C is almost three times higher than that of specimens

443 subjected to freeze–thaw cycles at -18 to +4°C, even though the latter specimens were
444 subjected to a longer freeze–thaw cycles. Based on these observations, it appears the
445 temperature ranges of thermal cycling have greater negative impact on pullout capacity than
446 the number of cycles applied.

447 Sheikh (2007) observed that the weakened bond between FRP and concrete under freeze–
448 thaw conditions was due to wider temperature cycling. Thus, it can be concluded that the high
449 and low temperature cycling widened the gaps at the head and GFRP-bar interface. While the
450 coefficient of thermal expansion of the heads and the bars was low, the difference was
451 nevertheless great enough during the expansion of the materials at low-temperature thermal
452 cycling to result in residual stresses that accentuated gap generation or widening. At high
453 thermal cycling, the moisture migrated into these gaps, reducing the shear strength at the
454 interface. The increased volume of the absorbed moisture during the low thermal cycling
455 further contributed to widening the gaps. This supports the findings by Koller et al. (2007),
456 who indicated that the bond deterioration in response to freeze–thaw cycles was due moisture
457 freezing and crystallizing between the FRP bar and concrete. Interestingly, the 11% decrease
458 is equal to total decrease in the pullout capacity observed for the headed bars exposed to the
459 alkaline solution and freeze–thaw cycling at 18°C to -4°C. Since the headed bars were
460 embedded in moist concrete before being subjected to freeze–thaw cycles at -30 to +30°C, the
461 bond at the bar–head interface was affected, not only by high temperature cycling, but also by
462 the pore water of the surrounding moist concrete.

463 **Effect of Exposure to an Alkaline Solution and Sustained Loading**

464 The headed GFRP bars conditioned for 60 days in an alkaline environment and subjected to
465 sustained loading at 60°C failed at an average load of 109.9 kN, which is 79.4% of the control
466 specimens. The 20% lower pullout capacity is significantly higher than that of group B
467 specimens, indicating that the induced tensile loading significantly affected pullout strength.

468 Moreover, the sustained tensile loading of 3000 microstrains further decreased the pullout
469 strength by 14%.

470 Shahidi et al. (2006) indicated that a decrease in bond performance under sustained loading
471 can be caused by bar slip. This can be clearly seen with E-5-35-S-1 in our study, since the
472 grooves fastening the head to the bar were damaged during failure. Moreover, the sustained
473 loading caused microcracking in the head and bar surface, which served as a passage for the
474 alkaline solution and the migration of high-pH solutions and moisture into the bar–head
475 interface, thereby reducing the shear strength. Benmokrane et al. (2002) showed that alkaline
476 ions and moisture could penetrate or diffuse, under sustained stress levels, through the resin
477 or through the cracks and voids to the interphases and the fibers. They further concluded that
478 the penetration of alkaline ions into the GFRP bars increased with exposure time, which
479 further reduced the mechanical properties of the aged GFRP bars. Thus, the shear failure of
480 the grooves observed for headed bars exposed to this condition was due to moisture
481 absorption through the cracks, which damaged the resin-rich grooves at the bar surface.

482 From these experimental results, it can be concluded that the alkaline solution and
483 sustained loading at 60^{o}C primarily affected the pullout strength and the retained pullout
484 capacity of the headed GFRP bars. The lower pullout capacity was generally small, indicating
485 that the damage was confined to the bar–head interface, while the head and bar retained their
486 initial material properties. In fact, Benmokrane et al. (2002) did not observe any significant
487 difference in the residual tensile strength of GFRP bars subjected to a NaOH solution (pH of
488 13.1) under a stress level of 30% over 60 days. After being exposed for 60 days, the pullout
489 retention was just below 80%.

490 The bar slippage observed for all conditioned specimens clearly demonstrated that the
491 shear strength at the bar–head interface was affected by exposure to the alkaline and freeze–

thaw environments. This conclusion was supported by scanning electron microscopy (SEM) observation and analysis, which is presented in Section 6.

Comparison of Straight and Headed GFRP Bars

Islam et al. (2015) concluded that GFRP bars with a headed end showed significantly higher pullout strength compared to straight end bars. In their study, the ribbed GFRP bars with headed ends developed 52% of the short-term tensile strength. In contrast, the newly developed headed GFRP bars achieved up to 63% and 53% of the guaranteed tensile strength for Nos. 5 and 6 bars, respectively, as shown in Table 3. This indicates that the materials and head interface configuration improved the mechanical interlocking between the head and FRP bar. Moreover, the pullout capacity of the headed GFRP bar was approximately 90% higher than the pullout capacity of the sand-coated GFRP bar without a head. Ahmed and Benmokane (2009) achieved only a maximum stress of 385 MPa (pullout load of 76.75 kN) for the sand-coated GFRP bar embedded 100 mm into a 35 MPa concrete. Robert and Benmokrane (2010) reported a bond strength of 15 MPa for 19 mm diameter, sand-coated GFRP bars embedded in a 55 MPa concrete to a length of 100 mm. This gives a pullout load of around 90 kN or develops a tensile stress of 315 MPa, which is only half the average tensile stress developed by the headed GFRP bars.

The actual stress developed in the headed GFRP bars was more than twice the design values, indicating that, even without additional embedment length, it was sufficient to develop the design tensile strength of the GFRP bars. CAN/CSA-S806 (2012) indicates that the maximum stress in GFRP bars under load at the serviceability limit state shall not exceed the 25% of the characteristic tensile strength or around 275 MPa. Moreover, the test results of the conditioned headed GFRP bars indicated that the stress values at failure was at least 2.2 times the allowable stress limit according to CAN/CSA-S6-14 (2014). While it would be difficult to report the nominal bond stress of the head and bar interface for unconditioned samples due to

517 the nature of the observed failure of these specimens, it can be deduced that the bond stress of
518 head–bar interface was at least 28.2 MPa based on the average failure load of specimen C-5-
519 35-S. Even when exposed to the alkaline solution and under sustained loading, the average
520 stress at failure in No. 5 headed GFRP bars was 555 MPa. This represents 46% of the tensile
521 strength of the GFRP bars and is approximately 1.38 times the yield strength of the 400 MPa
522 steel bar. These results, however, also demonstrate that head geometry and the head–bar
523 interface can still be further optimized to reach the expected loading efficiency with bar
524 rupture.

525 **SEM and DSC Observations**

526 Robert and Benmokrane (2010) indicated that there will be a loss of bond if any resin or fiber
527 degradation occurs at the interface, which could also affect the structure's durability. Thus,
528 cross sections of the headed bar from groups A, B, and C were cut, prepared, and analyzed
529 with a Hitachi SEM. The GFRP bar and head were observed under scanning electron
530 microscopy (SEM) to more accurately assess the state of the bar–head interface. Moreover,
531 this was done to detect the presence of any degraded areas or head detachment, and to provide
532 an explanation for the slight decrease in the pullout strength of the specimens exposed to the
533 alkaline solution and freeze–thaw cycles compared to the control specimens. Similarly, the
534 rate of absorption of the conditioned specimens was measured and analyzed with a TA
535 Instruments Q10 differential scanning calorimeter (DSC) to measure the glass transition
536 temperature after conditioning. Robert and Benmokrane (2010) suggested that a decrease in
537 T_g in the conditioned samples indicates irreversible chemical degradation and reduced
538 material durability.

539 ***Unconditioned Specimens***

540 Figures 6a and 6b present SEM micrographs of the cross section of the head from the control
541 specimens (Group A). The figure shows that the head material contains glass fibers oriented

along the bar axis. There was no noticeable gap at the bar–head interface, indicating excellent adhesion between them. The presence of pores in limited numbers can, however, be observed from the figure, probably caused by air trapped in the resin. Moreover, a few gaps in the bar–head interface can be observed indicating they existed prior to mechanical loading and environmental conditioning.

Samples Conditioned in a High pH Solution

The glass transition temperature measured by DSC of the head conditioned under high pH (Group B) was an average of 145°C. This is slightly higher than the T_g for the reference material (140°C). Similarly, the rate of absorption at saturation was 1.02%, indicating that no change in the material composition compared to the unconditioned samples (1.11%). Furthermore, infrared spectroscopy (FTIR) of the head surface directly exposed to the high pH solution revealed no damage. Figure 7 clearly shows no differences between the infrared spectra of the control and conditioned specimens.

Figures 6c and 6c show a general view and close view, respectively, of the bar–head interface after the conditioning in high pH solution. While a space can be observed between the head and bar, the width varies depending on the measurement location. In a specimen taken from the same cut, a gap of about 5 μm was observed, while it was up to 10 μm in another location. Thus, it can be concluded that the small gaps observed in the unconditioned specimens served as a passage for the alkaline solution. It should be noted that there are also locations where there are no gaps between the interfaces. Furthermore, it has not been established that all the heads were identical. In addition, the mechanical action involved in preparing the sample for microscopy might have modified the interface, if it weren't strong enough. Thus, the widened space observed at the interface may or may not be entirely caused by conditioning. More importantly, the very narrow gap at the interface and the fact that it is

not present throughout the entire sample, indicates that it did not significantly affect the pullout capacity of the headed GFRP bar, as highlighted in the preceding section.

Samples Subjected to Freeze–Thaw Cycles

The glass transition measurement by DSC of the heads exposed to freeze–thaw cycles at -18°C to +4°C (Group C) was 144°C. This is very close to the T_g of the unconditioned samples (140°C), indicating that no plasticizing effect or chemical degradation occurred after subjecting the headed GFRP bars to temperature cycling. Similarly, the rate of absorption at saturation was 1.07%, indicating that no change in material composition compared to the unconditioned samples (1.11%).

Figures 6e and 6f contain electron-microscopy photographs at the bar–head interface of the samples after freeze-thaw conditioning. Figure 6e shows the interface at 250 times magnification, revealing the appearance of a very thin opening between the bar and head. The higher magnification (500 times) of the interface in Figure 6f shows that the opening is around 2 μm, which is scaled based on the glass-fiber diameter of 20 μm. Robert and Benmokrane (2010) explained that the loss of bond strength between an FRP bar and concrete can be due to reduced shear strength at the concrete–sand-coating interface due to moisture saturation of the concrete and moisture absorption in the sand coating. The DSC measurement indicates otherwise for the headed GFRP bars. The reduction in the pullout capacity of the headed GFRP bars can be due to moisture ingress at the small gap between the bar–head interface. Under freeze–thaw cycles at high and low temperatures, this gap increased, resulting in reduced pullout strength of the headed reinforcement.

CONCLUSIONS

A new type of headed GFRP bar was assessed in this study. Several parameters were considered, including the confinement effect by spiral reinforcement, bar diameter, and concrete compressive strength to evaluate the pullout capacity of the headed bars. Moreover,

591 the long-term performance of the headed GFRP bars when exposed to alkaline solution,
592 freeze–thaw cycles, and combined alkaline exposure and sustained loading were assessed.
593 Based on the results of this study, the following conclusions were drawn:

594 1. The polyphthalamide with short glass fibers is a suitable material for the headed ends.
595 The water absorption, coefficient of thermal expansion, and glass transition
596 temperature of this material was compatible to that of sand-coated E-glass/vinyl ester
597 GFRP bars. Moreover, this material had very good adhesion to GFRP bars and created
598 an intact interface resulting in a high pullout capacity.
599 2. The head geometry and interface configuration improved the mechanical interlock to
600 the bar surface, resulting in the GFRP bars developing high tensile strength. Up to
601 63% and 53 % of the guaranteed tensile strength were achieved with the 15.9 mm and
602 19 mm diameter bars, respectively. This corresponds to a tensile stress of 750 and
603 626 MPa, respectively, which is approximately 90% higher than the pullout capacity
604 of the straight GFRP bars. These stress values represent 1.5 to 1.8 times the yield
605 strength of the steel bars.
606 3. The spiral steel reinforcement provided sufficient confinement of the concrete block
607 and increased the pullout capacity of the headed GFRP bars by 13% to 15%. It
608 prevented the blowout of the concrete, resulting in the headed GFRP bars achieving
609 the maximum pullout capacity and then failing due to the breakage of the headed ends.
610 4. An increase in bar diameter decreased the pullout capacity of the headed GFRP bars
611 due to the decreased net area of the head bearing on the concrete. The reduction in
612 pullout resistance between the 19 mm and 15.9 mm diameter headed bars was 14% to
613 16%.
614 5. The concrete compressive strengths considered in this study had no significant effect
615 on the pullout capacity of the headed GFRP bars. Increasing the compressive strength

from 35 to 47 MPa only increased the pullout capacity by 4% to 6%. This can be attributed to concrete-block confinement and the pullout capacity being governed by head breakout, followed by bar slippage with tensile splitting of the concrete.

6. The retained pullout strength of the headed GFRP bars was 93% and 96% with exposure to an alkaline solution (pH of 12.5) and 500 freeze–thaw cycles at -18°C to +4°C, respectively, compared to the unconditioned specimens. The conditioned specimens failed due to bar slippage with the bar surface grooves remaining intact.
7. The high- and low-temperature cycling had a more detrimental effect on the pullout capacity of headed GFRP bars than exposure to the alkaline solution. The pullout retention of the specimens exposed to freeze–thaw cycling at +30 to -30°C was 88.9%. This decrease in the shear strength at the bar–head interface was due to gap widening during material contraction at low temperature and migration of concrete pore water at high temperature.
8. The exposure to the alkaline solution and sustained loading for 60 days at 60°C primarily affected the pullout capacity and retention of the headed GFRP bars. The sustained loading further decreased the pullout strength by as much as 14%. The headed GFRP bars exposed to this type of environmental conditions retained a pullout capacity of 79.4%. These specimens failed as the result of shear failure of the grooves on the bar surface, resulting in slippage from the head.
9. SEM and DSC observations showed no material changes in the head and GFRP bars after exposure to the alkaline solution and freeze–thaw cycling. There were no changes in moisture absorption or glass transition temperature. Moreover, FTIR did not reveal any significant changes in specimen chemical structure after exposure to the highly alkaline solution.

10. Based on the SEM observations, it can be concluded that proper casting of the head and GFRP bars is essential in protecting them from environmental exposure. Moisture will ingress via even the narrowest gap in the bar–head interface, thereby reducing its shear strength. Despite the widening of the gap during exposure, the minimum retained pullout strength of the headed GFRP bars was just below 80% after being subjected to the alkaline solution and sustained loading at 60^{o}C for 60 days, which is significantly more severe than conditions anticipated in the field. This reduction is lower than the environmental reduction coefficient (0.70) required by several codes.

The results of this study prove that the new headed GFRP bars have suitable physical, mechanical, and durability properties for use as primary and secondary reinforcement in concrete bridge elements and structures. The tested product is currently used by the Ministries of Transportation in Quebec and Ontario.

Acknowledgements

The authors wish to express their gratitude and sincere appreciation to the Natural Sciences and Engineering Research Council of Canada (NSERC), the NSERC Research Chair in Innovative FRP Reinforcement for Concrete Structures, the Fonds de recherche du Québec en nature et technologies (FRQ-NT), and the Ministry of Transport Quebec for financing this research work. The material support from Pultrall Inc. (Thetford Mines, Quebec, Canada) and the technical assistance from the staff of the Structural Laboratory in the Department of Civil Engineering, Faculty of Engineering at the University of Sherbrooke are also gratefully acknowledged. The third author is quite appreciative of the scholarship granted by the Australian Government Endeavour Research Fellowships, enabling him to undertake his research and professional development at the University of Sherbrooke.

663 **References**

664 Ahmed, E., El-Sayed, A. K, El-Salakawy, E.F., Benmokrane, B., (2010). "Bend Strength of
665 FRP Stirrups: Comparison and Evaluation of Testing Methods." *ASCE Journal of*
666 *Composites for Construction*, Vol. 14, No. 1, Jan./Feb., pp. 3-10.

667 Al-Dulaijian, S., Al-Zahrani, M., Nanni, A., and Boothby, T.E. (2001). "Effect of
668 environmental pre-conditioning on bond of FRP reinforcement to concrete." *Journal of*
669 *Reinforced Plastics and Composites*, 20(10), 882-890.

670 Alves, J., El-Ragaby, A. and El-Salakawy, E. (2011). "Durability of GFRP bars' bond to
671 concrete under different loading and environmental conditions." *Journal of Composites*
672 *for Construction*, 15(3), 249-262.

673 American Concrete Institute (2008). Metric specification for carbon & glass fiber-reinforced
674 polymer bar materials for concrete reinforcement. ACI-440.6M-08, Farmington Hills,
675 Michigan, USA.

676 American Concrete Institute (2012). Guide test methods for fiber-reinforced polymer, ACI
677 440.3R-12, Farmington Hills, Michigan, USA.

678 American Concrete Institute (2015). Guide for the design and construction of concrete
679 reinforced with FRP bars, ACI 440.1R-15, Farmington Hills, Michigan, USA.

680 ASTM Standard D570 − 98 (2010). Standard test method for water absorption of plastics.
681 *ASTM D570 − 98,* ASTM International, West Conshohocken, Philadelphia, Pa 19103.

682 ASTM Standard E1131 - 08(2014). Standard test method for compositional analysis by
683 thermogravimetry. *ASTM E1131 - 08,* ASTM International, West Conshohocken,
684 Philadelphia, Pa 19103.

685 ASTM Standard D3171 Standard Test Methods for Constituent Content of Composite
686 Materials, American Society for Testing and Materials, Conshohocken, USA, 2011. p.
687 13.

688 ASTM E831 (2012). Standard Test Methods for Linear Thermal Expansion of Solids
689 Materials by Thermo-Mechanical Analysis, American Society for Testing and
690 Materials, Conshohocken, USA, 2012. p. 4.
691 ASTM Standard D5336 − 15 (2015). Standard classification system and basis for
692 specification for polyphthalamide (PPA) injection molding materials. *ASTM D5336 −*
693 *15,* ASTM International, West Conshohocken, Philadelphia, Pa 19103.
694 Azimi, H., Sennah, K., Tropynina, E., Goremykin, S., Lucic, S., and Lam, M. (2014).
695 "Anchorage capacity of concrete bridge barriers reinforced with GFRP bars with headed
696 ends." *Journal of Bridge Engineering,* 19(9), 1-15.
697 Bank, L.C., Puterman, M., and Katz, A. (1998). "The effect of material degradation on bond
698 properties of fiber reinforced plastic reinforcing bars in concrete." *ACI Materials*
699 *Journal*, 95(3), 232-243.
700 Benmokrane, B., Wang, P., Ton-That, T., Rahman, H., and Robert, J.F. (2002). "Durability of
701 glass fibre reinforcing bars in concrete environment." *Journal of Composites for*
702 *Construction*, 6(3), 143-153.
703 Benmokrane, B., El-Salakawy, E., El-Ragaby, A., and Lackey, T. (2006). "Designing and
704 testing of concrete bridge decks reinforced with glass FRP bars." Journal of Bridge
705 Engineering, 11(2), 217-229.
706 Benmokrane, B., Tighiouart, B., and Chaallal, O. (1996). "Bond strength and load distribution
707 of composite GFRP reinforcing bars in concrete." *ACI Material Journal*, 93(3), 246–
708 253.
709 Canadian Standards Association (CSA). (2015). "Specification for fibre-reinforced
710 polymers." CAN/CSA-S807, Rexdale, Ontario, Canada.

711 Canadian Standards Association (CSA). (2012). "Design and construction of building
712 structures with fibre-reinforced polymers." CAN/CSA-S806-12, Rexdale, Ontario,
713 Canada.
714 Canadian Standards Association (CSA). (2014). "Canadian highway bridge design code—
715 Section 16, updated version for public review." CAN/CSA-S6-14, Rexdale, Ontario,
716 Canada.
717 Cosenza, E., Manfredi, G. and Realfonzo, R. (1997). "Behaviour and modelling of bond of
718 FRP rebars to concrete." *Journal of Composites for Construction,* 1(2), 40-51.
719 Davalos, J.F., Chen, Y. and Ray, I. (2008). "Effect of FRP bar degradation on interface bond
720 with high strength concrete." *Cement and Concrete Composites,* 30, 722-730.
721 El-Salakawy, E.F., Benmokrane, B. and Brière, F. (2005). "Glass FRP composite bars for
722 concrete bridge barriers." *Journal of Science and Eng. of Composite Materials*, 12(3),
723 167-192.
724 Harajli, M. and Abouniaj, M. (2010). "Bond performance of GFRP bars in tension:
725 experimental evaluation and assessment of ACI 440 guidelines." *Journal of Composites*
726 *for Construction,* 14(6), 659-668.
727 Homam, S.M. and Sheikh, S.A. (2014). "Durability of fibre reinforced polymers used in
728 concrete structures." *Proceedings of the 3rd International Conference on Advanced*
729 *Materials in Bridges and Structures*, Ottawa, Canada, 15-18 August, 751-758.
730 Islam, S., Afefy, H.A., Sennah, K., and Azimi, H. (2015). "Bond characteristics of straight-
731 and headed-end, ribbed-surface, GFRP bars embedded in high-strength concrete."
732 *Construction and Building Materials,* 83, 283-298.
733 Koller, R., Chang, S. and Xi, Y. (2007). "Fiber-reinforced bars under freeze-thaw cycles and
734 different loading rates." *Journal of Composite Materials,* 41(1), 5-25.

735 Manalo, A.C., Benmokrane, B., Park, K., and Lutze, D. (2014). “Recent developments on
736 FRP bars as internal reinforcement in concrete structures”. *Concrete in Australia*, 40(2),
737 46-56.
738 Mashima, M., and Iwamoto, K. (1993). "Bond characteristics of FRP rod and concrete after
739 freezing and thawing deterioration." *Proc., Int. Symp. on Fiber-Reinforced-Plastic*
740 *Reinforcement for Concrete Struct.*; ACI SP-138, A. Nanni and C. W. Dolan, eds.
741 Micelli, F. and Nanni, A. (2004). “Durability of FRP rods for concrete structures.”
742 *Construction and Building Materials*, 18, 491-503.
743 Okelo, R. and Yuan, R.L. (2005). “Bond strength of fibre reinforced polymer rebars in normal
744 strength concrete.” *Journal of Composite for Construction,* 9, 203-213.
745 Ozbolt, J., Eligehausen, R., Periskic, G., and Mayer, U. (2007). “3D FE analysis of anchor
746 bolts with large embedment depths.” *Engineering Fracture Mechanics,* 74 (1-2), 168-
747 178.
748 Platt, D. (2003). “Engineering and high performance plastics.” *A Rapra Market Report*; Rapra
749 Technology Limited, Shropshire, UK.
750 Reza Esfahani, M., Rakhshanimehr, M. and Roohollah Mousavi, S. (2013). “Bond strength of
751 lap-spliced GFRP bars in concrete beams.” *Journal of Composites for Construction,*
752 17(3), 314-323.
753 Robert, M. and Benmokane, B. (2010). “Effect of aging on bond of GFRP bars embedded in
754 concrete.” *Cement and Concrete Composites*, 32, 461-467.
755 Shahidi, F., Wegner, L.D. and Sparling, B.F. (2006). “Investigation of bond between fibre-
756 reinforced polymer bars and concrete under sustained loads.” *Canadian Journal of Civil*
757 *Engineering*, 33, 1426-1437.

Sheikh, S.A. (2007), "Effect of freeze-thaw climatic conditions on long-term durability of FRP strengthening systems", University of Toronto, Final report submitted to the Ministry of Transportation of Ontario, pp. 1-47.

Thomson, M.K., Jirsa, J.O., Breen, J.E., and Klinger, R.E. (2002), "Anchorage behaviour of headed reinforcement: Literature review", University of Texas at Austin, Final report submitted to the Texas Department of Transportation, Austin, Texas, pp. 1-102.

Tighiouart, B., Benmokrane, B. and Gao, D. (1998). "Investigation of bond in concrete member with fibre reinforced polymer (FRP) bars." *Construction and Building Materials*, 12, 453-462.

List of Tables

List of Figures

797
798

Table 1. Summary of conducted test methods to determine the physical properties of sand coated GFRP bars and their heads

Physical properties	Standard test method	Sand coated GFRP bar	Head
Cross sectional area	ASTM D7205	✓	N.A
Constituent content of composite materials	ASTM D 3171	✓	✓
Water absorption	ASTM D 570	✓	✓
CTE	ASTM E 831	✓	✓
Glass transition temperature	ASTM D 3418	✓	✓

Table 2. Mechanical properties of the straight GFRP bars

Bar Size	Nominal Diameter (mm)	Nominal Cross-Sectional Area (mm^2)	Area by Immersion Tests (mm^2)	Glass Content % weight	Tensile Strain (%)	*Tensile Modulus (MPa)	*Guaranteed Tensile Strength (MPa)
No. 5	15	198	227	83	1.89	62.6 ±2.5	1184
No. 6	20	285	341	83	1.71	64.7 ±2.5	1105

*Note: The tensile modulus and strength are calculated based on nominal cross-sectional area of the bar.

Table 3. Details of the specimens and summary of test results

Specimen Designation	Bar Diameter (mm)	Concrete Strength (MPa)	Confinement	Number of Specimens	Average Failure Load (kN)	Standard Deviation (kN)	Average Tensile Stress at Failure (MPa)	f_s/f_{ps} (%)	Mode of Failure
Reference Specimens									
A-5-35-N-#	15	35	No confinement	5	123	4.1	620	52.4	CB
A-5-35-S-#	15	35	With steel spiral	10	139	9.6	699	59.1	CSH
A-5-47-S-#	15	47	With steel spiral	10	149	4.1	750	63.3	CSH
A-6-35-N-#	20	35	No confinement	5	150	12.3	525	47.5	CB
A-6-35-S-#	20	35	With steel spiral	5	172	11.6	603	54.5	CSH
A-6-47-S-#	20	47	With steel spiral	10	179	14.0	627	52.9	CSH
Conditioned Specimens									
B-5-35-S-#	15	35	With steel spiral	3	129	7.0	652	55.1	BSH
C-5-35-S-#	15	35	With steel spiral	3	133	0.1	671	56.7	BSH
D-5-35-S-#	15	35	With steel spiral	3	117	4.0	622	52.5	BSH
E-5-35-S-#	15	35	With steel spiral	3	109	3.2	555	46.9	BSG

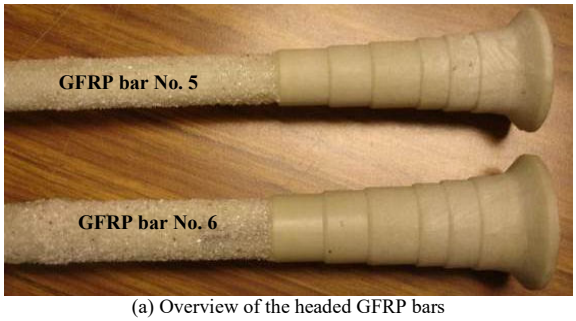

(a) Overview of the headed GFRP bars

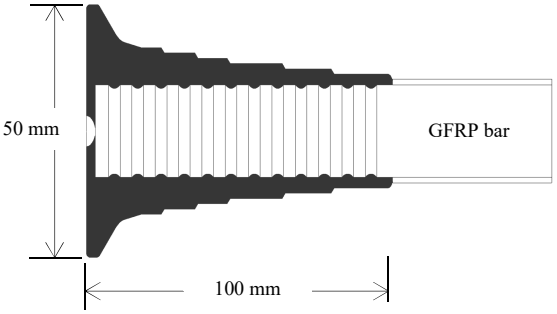

(b) Schematic diagram for the head and bar interface

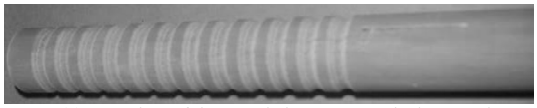

(c) Overview of the rounded grooves on the bar's end

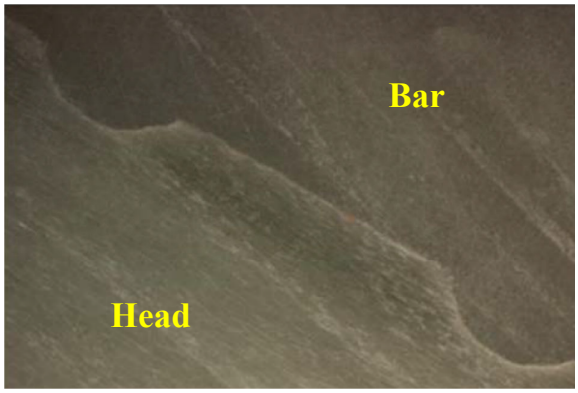

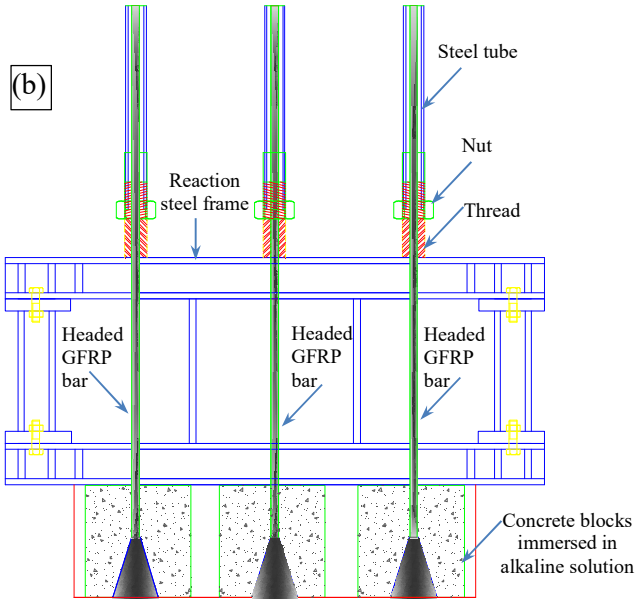

(a) CB

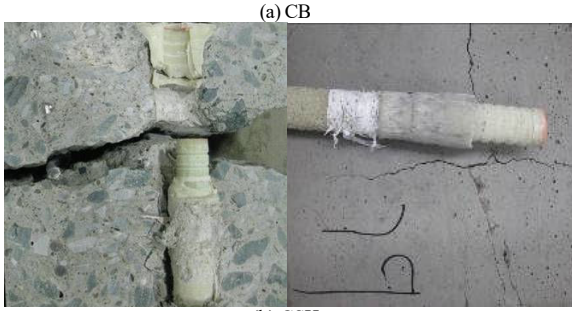

(b) CSH

(c) BSH

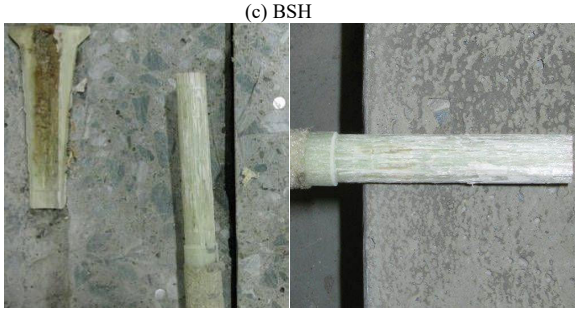

(d) BSG

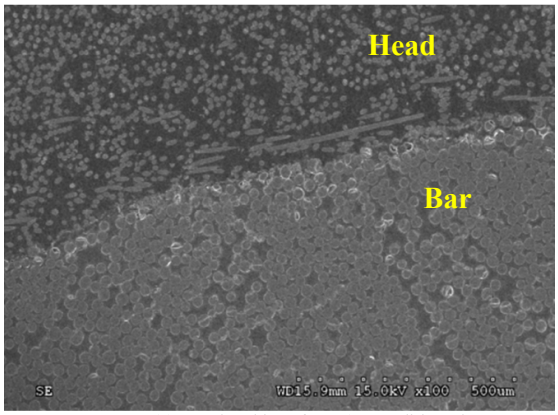

(a) Bar–head interface (unconditioned)

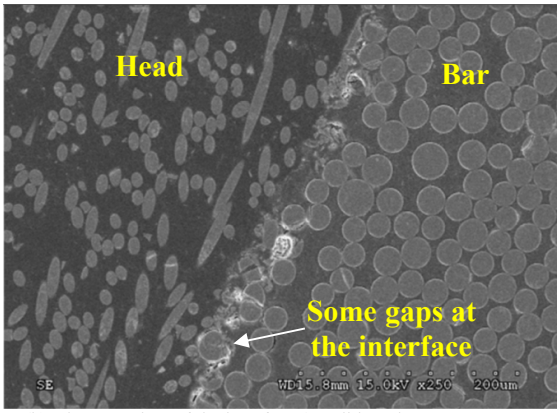

(b) Close-up view of the interface (conditioned)

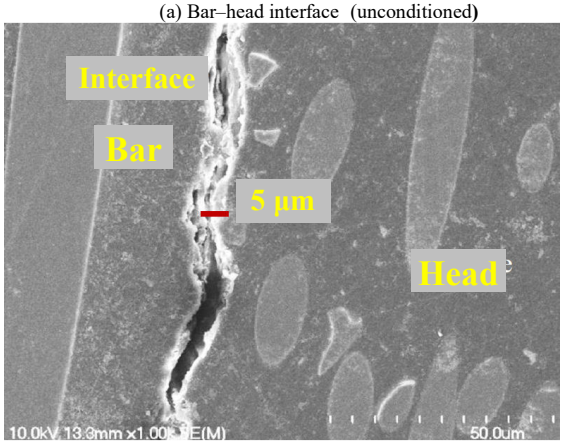

(c) Bar–head interface after exposure to an alkaline solution

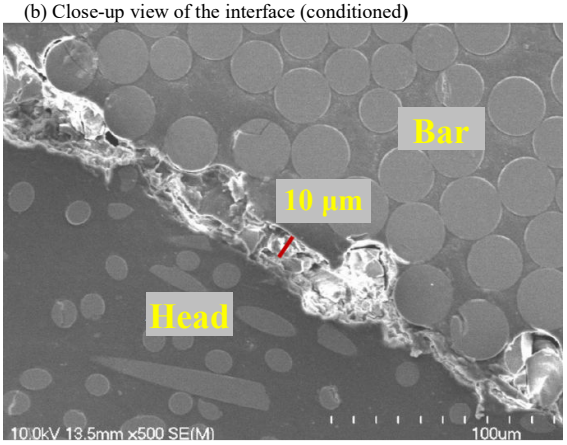

(d) Close-up view of the interface after exposure to an alkaline solution

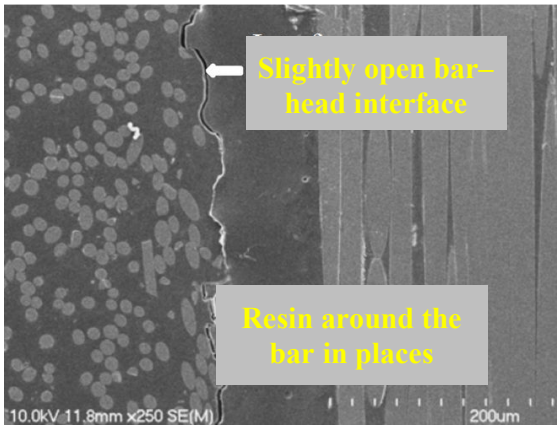

(e) Bar–head interface after freeze–thaw cycles

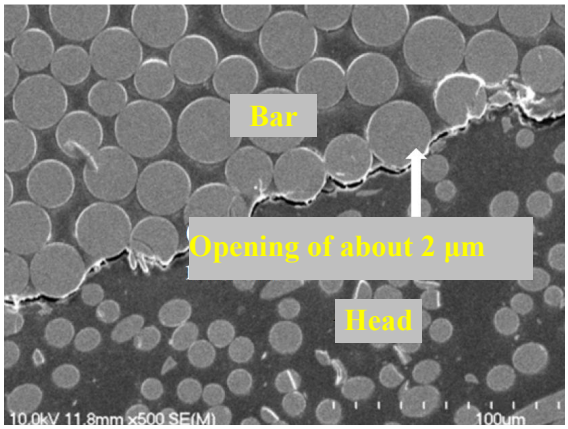

(f) Close-up view of the interface after freeze–thaw cycles

Figure

Click here to download Figure Fig. 7.pdf

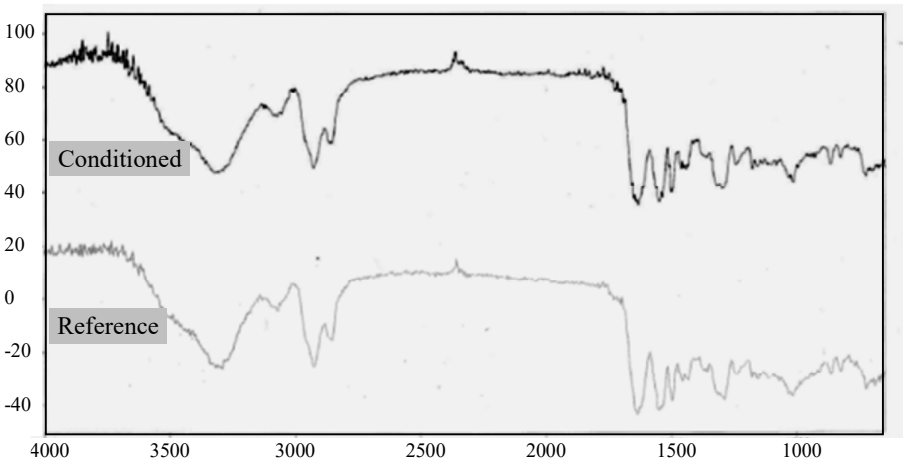

Figure Captions List